Electron Temperature and Thermal Conductivity Profile Measurements in the MST Reversed-Field Pinch

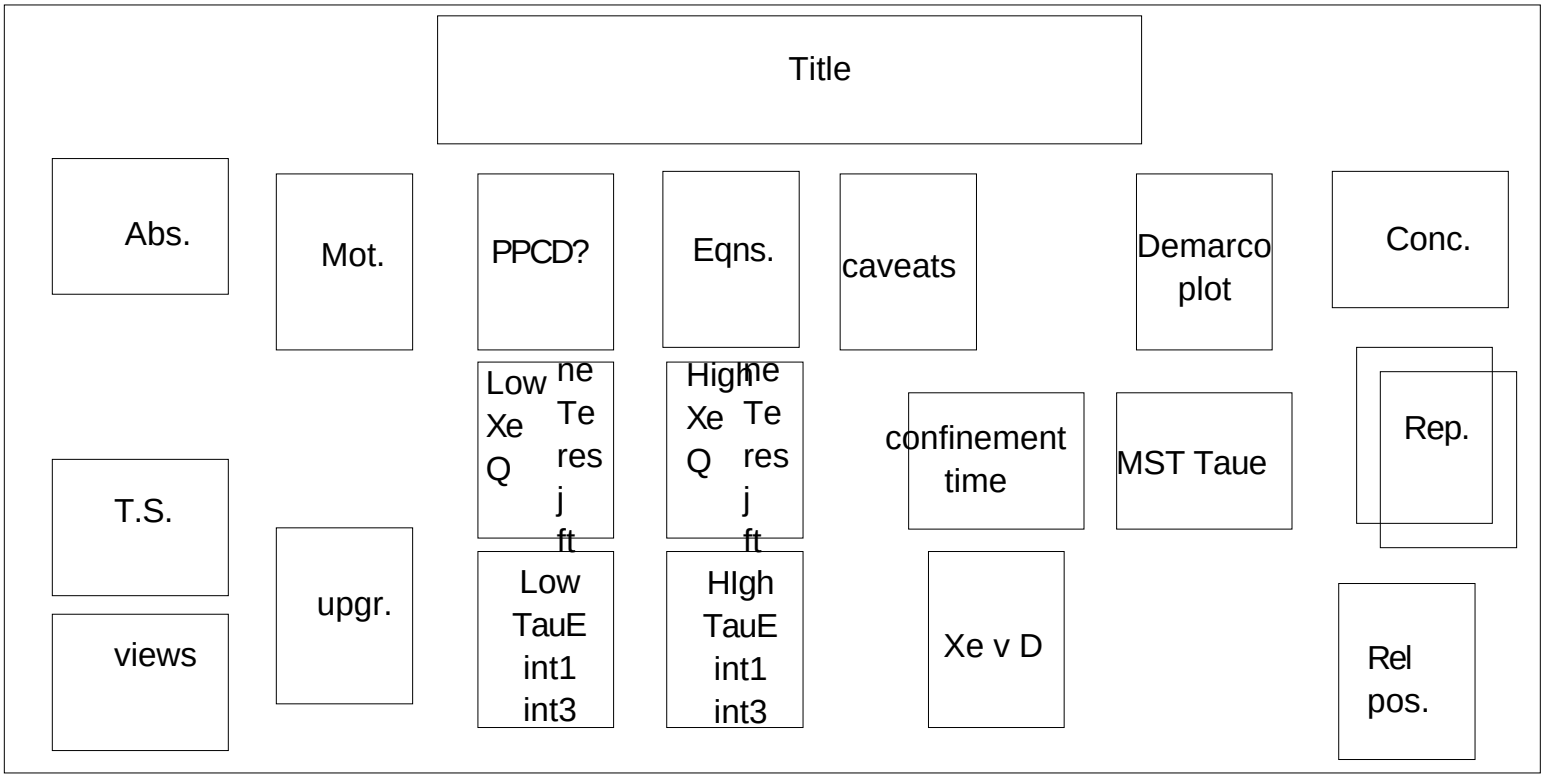

Electron Temperature and Thermal Conductivity Profile Measurements in the MST Reversed-Field Pinch.

T.M. Biewer, D.J. Holly,
J.K. Anderson, B.E. Chapman, N.E. Lanier, C.B. Forest
University of Wisconsin-Madison.

Recent modifications have extended the radial range of the MST Thomson scattering system. These improvements have yielded more reliable electron temperature profiles, which when coupled with FIR interferometric measurements of plasma density and MSTFIT equilibrium reconstructions, give an estimation of the electron thermal conductivity profile in MST. Measurements with pulsed poloidal current drive (PPCD) show how edge driven current effects the stored thermal energy of the plasma and improves the energy confinement time. Preliminary results show that $\tau_{E,e}$ increases from the MST standard time of 1 ms to roughly 4 ms during PPCD, based on neoclassical resistivity with a Z_{eff} of 1.9. Additionally, $\beta_{p,e}$ reaches a value of 15% during PPCD plasmas. These numbers represent a lower bound on τ_E and β_p because the effects of ions were not considered in these calculations.

This work was supported by the U.S. D.O.E.

Motivation

- The use of Pulsed Poloidal Currnt Drive (PPCD) has demonstrated improved confinement in the MST, based on central electron temperature measurements and a hypothesized profile shape.

- Recent upgrades of the Thomson Scattering system have allowed for measurements of the T_e profile in the MST out to r/a=0.88.

- These measurements, when coupled with density profiles from FIR Interferometry and MSTFIT reconstructed equilibriums, have made it possible to calculate the electron heat flux Q, the electron thermal conductivity X_e, and even the electron energy confinement time $\tau_{E,e}$.

- Z_{eff} is the parameter that remains largely unkown in the MST, and strongly affects the calculation of $\tau_{E,e}$.

- By varying the plasma current, we can examine the performance of PPCD in terms of global machine characteristics.

MST Thomson Scattering Diagnostic

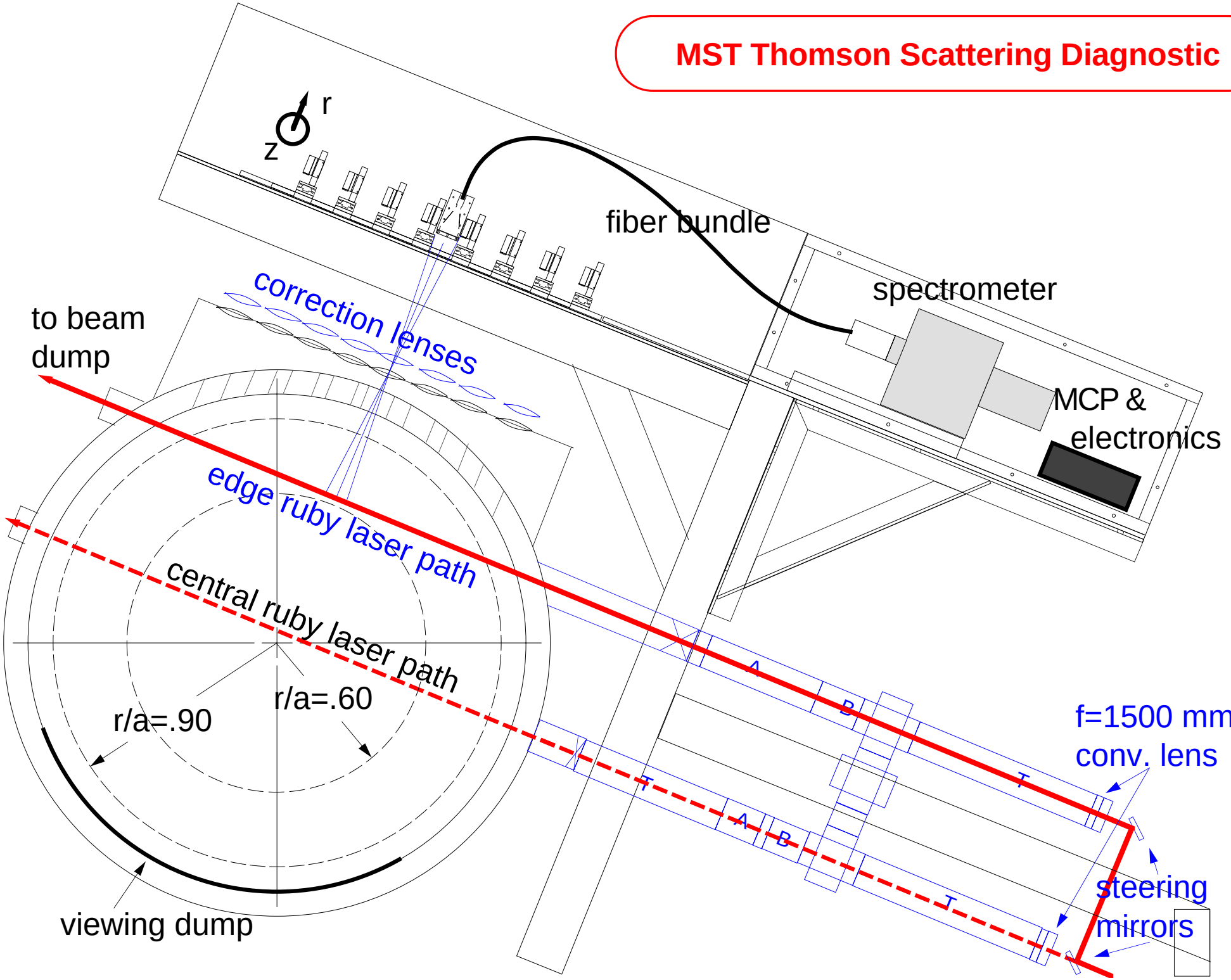

Thomson Scattering Views

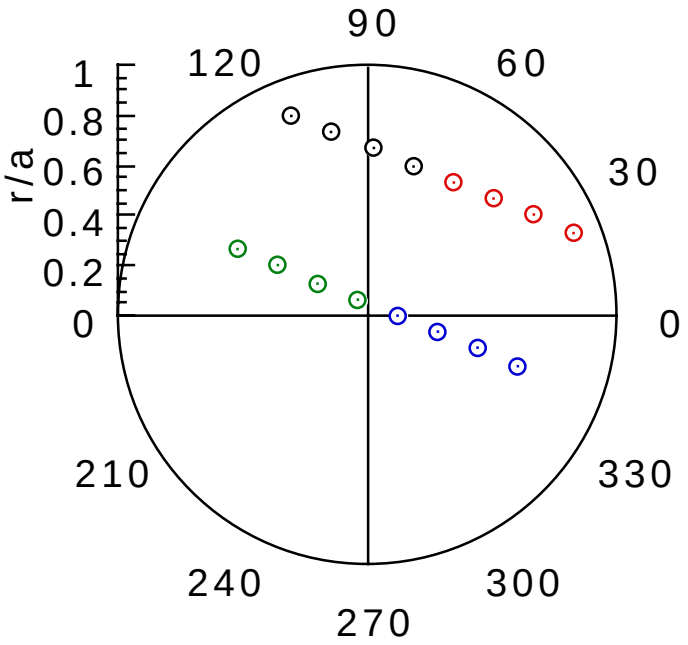

view	r/a	ϕ
1	0.627	-18.46
2	0.455	-16.93
3	0.283	-13.53
4	0.115	0
5	0.080	123.91
6	0.244	147.06
7	0.415	151.39
8	0.587	153.19
9	0.882	22.28
10	0.769	31.41
11	0.681	43.26
12	0.630	57.76
13	0.625	73.61
14	0.666	88.59
15	0.746	101.10
16	0.854	110.82

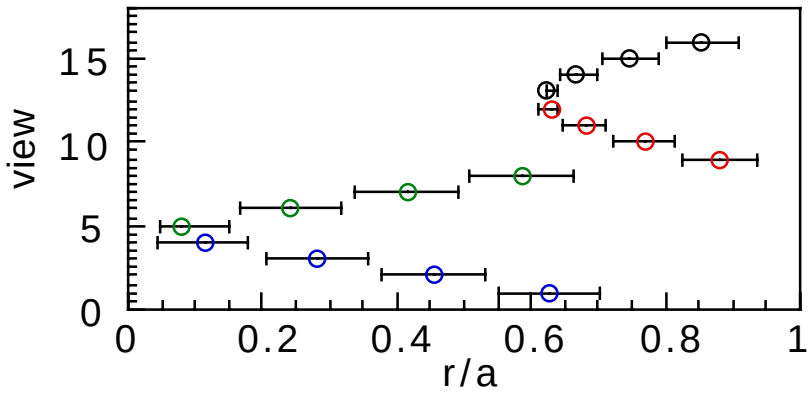

error bars indicate radial range of scattering volume on each view

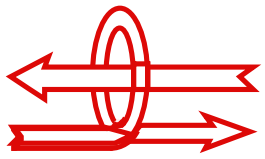

MST

An upgrade is underway to improve the resolution of the MST Thomson System

The current 5 wavelength channel MicroChannel Plate (MCP) detector will be replaced by an 11 channel Large Area Avalanch Photodiode Detector (LA APD) array. This will effectively double the wavelength range covered, and allow us to measure Thomson scattered photons on both sides of the ruby line, yielding a rudimentary estimation of the local current density.

Simulated Improvement

M.R. Stoneking
MST PLP 1181

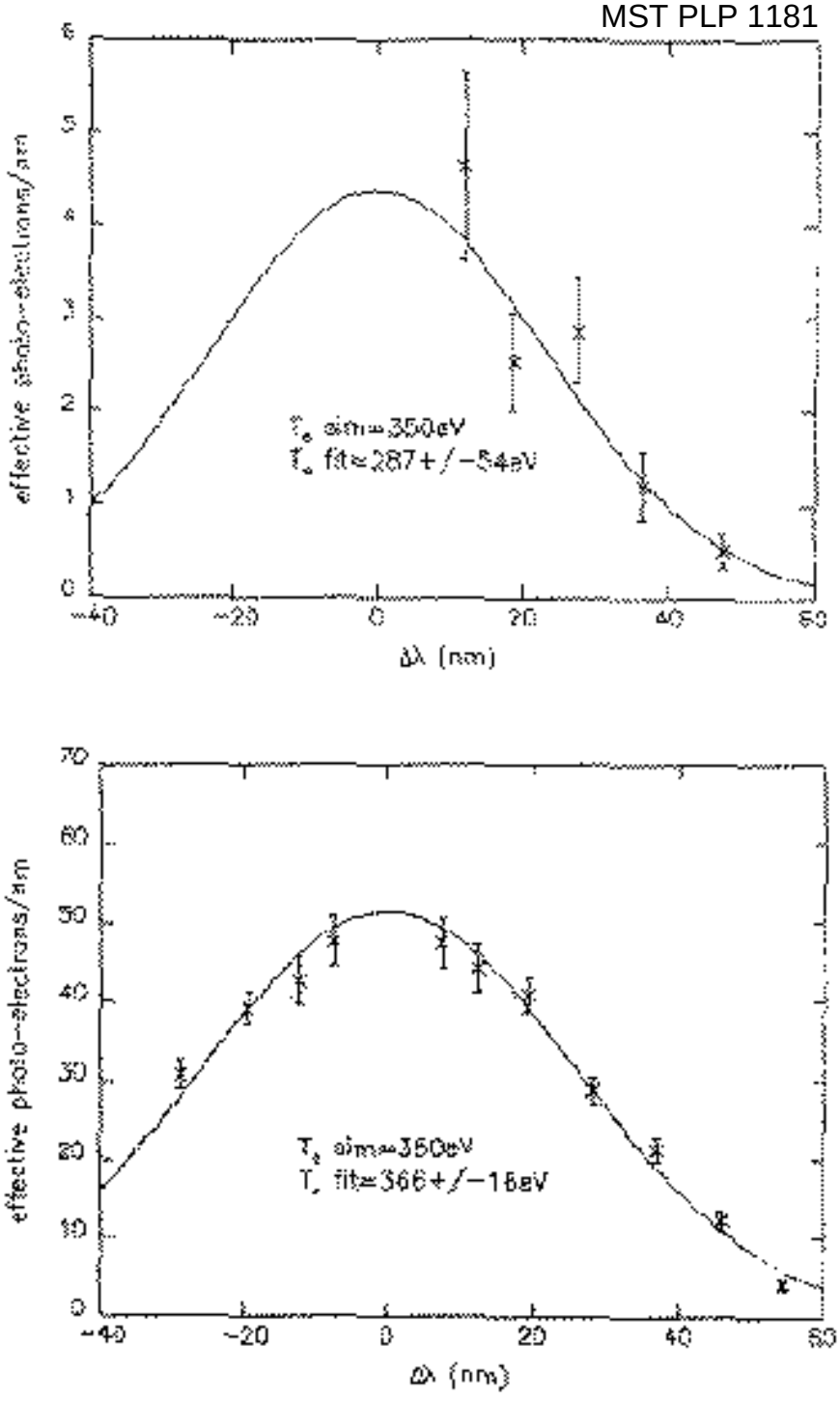

What is Pulsed Poloidal Current Drive?

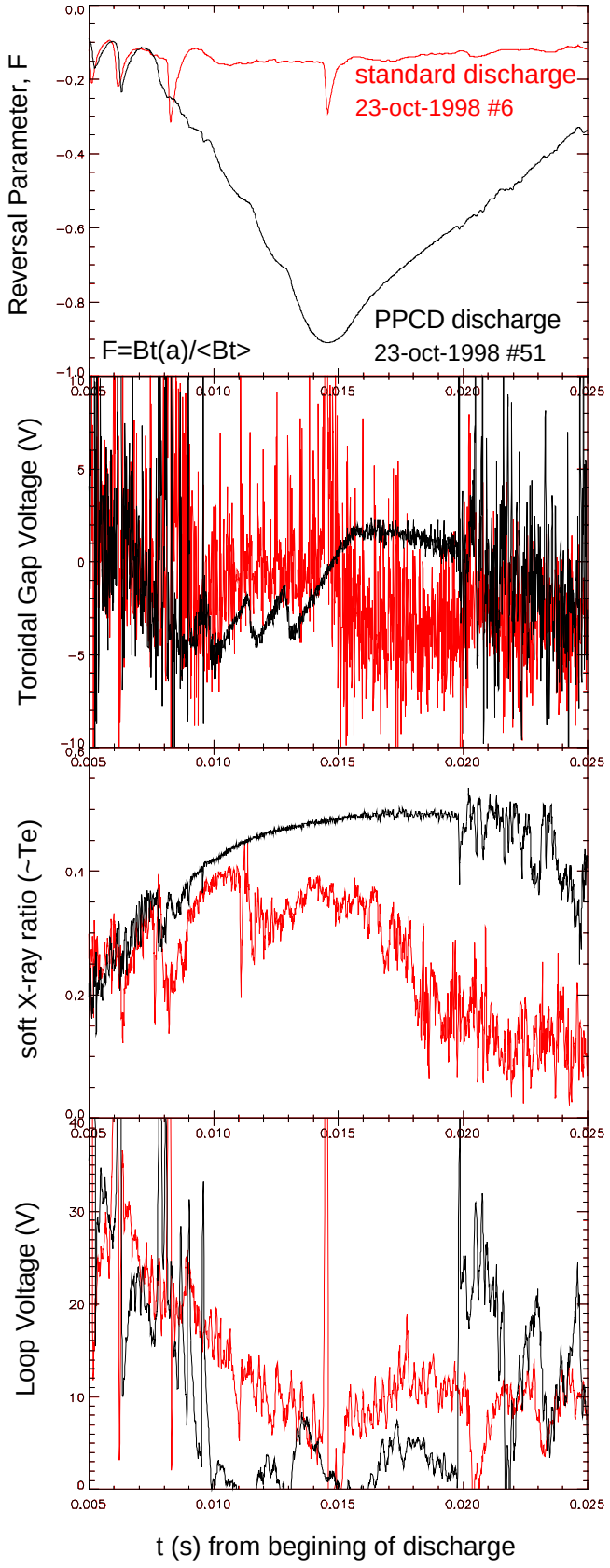

During a "normal" plasma discharge a series of 5 voltage pulses are applied to the MST shell to produce a magnetic field which is in the opposite sense to the established toroidal magnetic field, forcing flux out of the MST. This opposing B is thought to be due to a poloidally driven edge current.

PPCD is observed to improve machine performance. It is believed that magnetic modes in the MST derive their free energy from the gradient in the current profile, which is steepest at the edge. By inductively driving current in the edge, PPCD could reduce the gradient and remove free energy from the magnetic modes, resulting in decreased magnetic fluctuations and hence improved particle and energy confinement.

Calculation of Q and Xe

$$\frac{\partial}{\partial t}\left(\frac{3}{2}n_e T_e\right)+\nabla\bullet Q = S$$

$$\int\frac{\partial}{\partial t}\left(\frac{3}{2}n_e T_e\right)dV+\int\nabla\bullet Q dV=\int S dV\approx\int\eta j^2 dV - P_{rad} - P_{CX}$$

$$Q\approx\frac{\int\eta j^2 dV-\int\frac{\partial}{\partial t}\left(\frac{3}{2}n_e T_e\right)dV - P_{rad} - P_{CX}}{4\pi^2 R_0 r}$$

$$Q = -X_e n_e \nabla T_e - \frac{5}{2} D T_e \nabla n_e$$

$$\eta_{Neo}=\frac{\eta_{Sp}(ohm-m)}{1-f_t}\approx 5.2x10^{-5}\frac{Z_{eff}\ln\Lambda}{T_e^{3/2}(eV)}\frac{1}{(1-f_t)}$$

$$X_e\approx\frac{1}{n_e\nabla T_e}\left(\frac{-\int\eta j^2 dV+\int\frac{\partial}{\partial t}\left(\frac{3}{2}n_e T_e\right)dV}{4\pi^2 R_0 r}-\frac{5}{2}DT_e\nabla n_e\right)$$

Caveats on X_e, Q, τ_E

- **The effects of fast electrons are totally neglected.**

- **We have made the working supposition that D~0 m^2/s.**

- **P_{rad} and P_{CX} are assumed to be negligible** for this calculation. Prad at the edge of MST can be on the order of 10% of the estimated ohmic input power.

- **We can only estimate Z_{eff}.** The value used here (1.9) is based on measurements made in 1996 from NIR bremstrahlung at similar currents. Though that data was found to be contaminated by line radiation, it represents the best estimate of Z_{eff} in the MST.

- $\dot{w} = \frac{\partial}{\partial t}\left(\frac{3}{2} n_e T_e\right)$ **is assumed to be small**, and so has been neglected. The central density trace measured by CO_2 interferometry and the central T_e trace as estimated by the soft x-ray ratio of two beryllium filters indicate that both the density and temperature have reached steady state (under PPCD) at the time the Thomson scattering measurement of T_e is made (t=0 below).

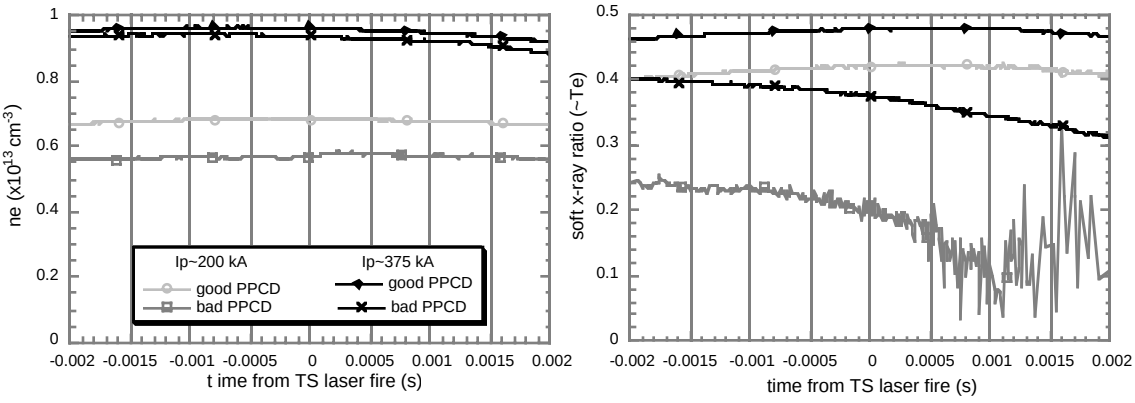

- The SXR ratio is proportional to temperature, for the most part, but is also sensitive to density and can be contaminated by line radiation. Furthermore, at these temperatures the SXR ratio is saturating in the nonlinear region of its sensitivity, and so may not be a good indication of the behavior of T_{e0}.

PPCD Leads to Lower Electron Thermal Conductivity

Ip~375 kA

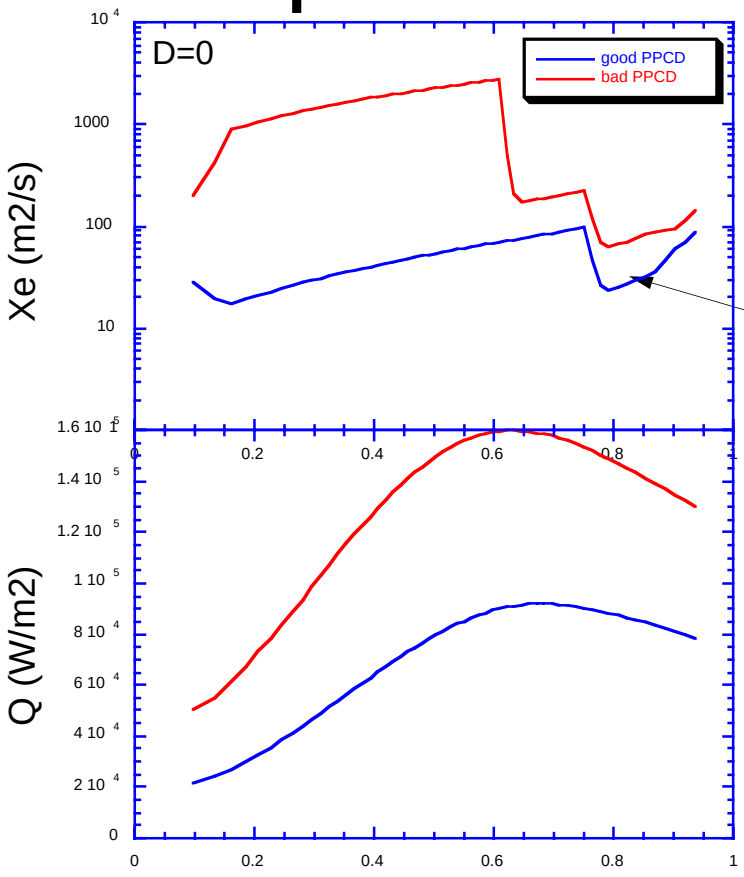

Xe is reduced by a factor of 50 in the core and by a factor of 5 at the edge.

Better Xe at the edge leads to an energy transport barrier for electrons.

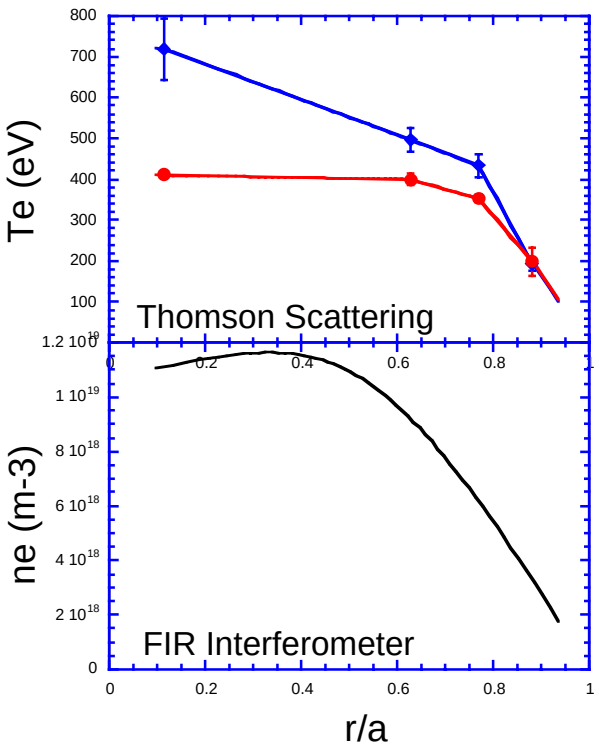

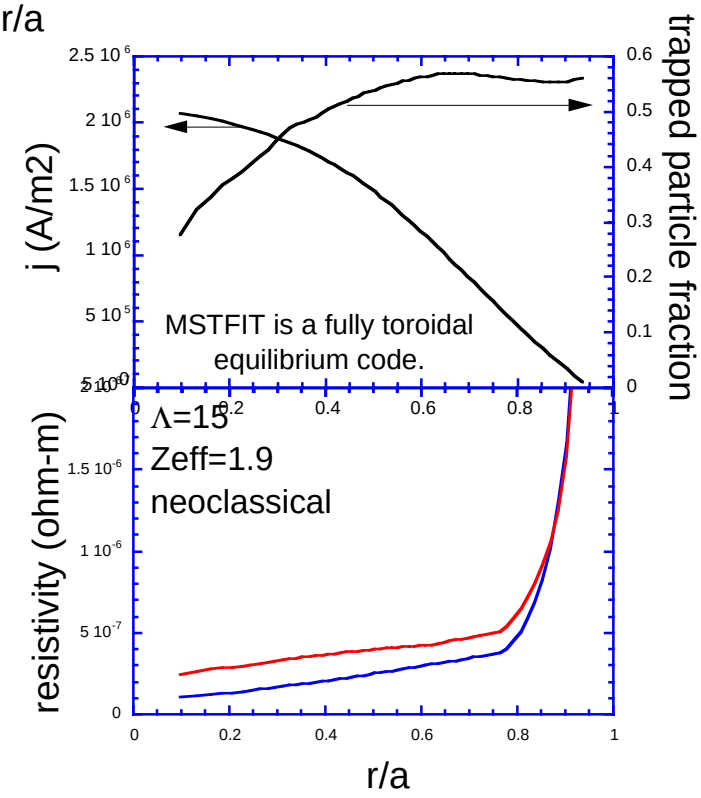

PPCD Increases Energy Confinement Time for Electrons to ~3 ms (w/est. ohmic power)

Ip~375 kA

Energy Confinement Time for electrons

$$\tau_{E,e} \approx \frac{\int \frac{3}{2} n_e T_e \frac{\partial V}{\partial r} dr}{\int \eta j^2 \frac{\partial V}{\partial r} dr} \quad \text{(ms)}$$

Ohmic Input Power

$$\int \eta j^2 \frac{\partial V}{\partial r} dr \quad \text{(Watts)}$$

Stored Thermal Energy

$$\int \frac{3}{2} n_e T_e \frac{\partial V}{\partial r} dr \quad \text{(Joules)}$$

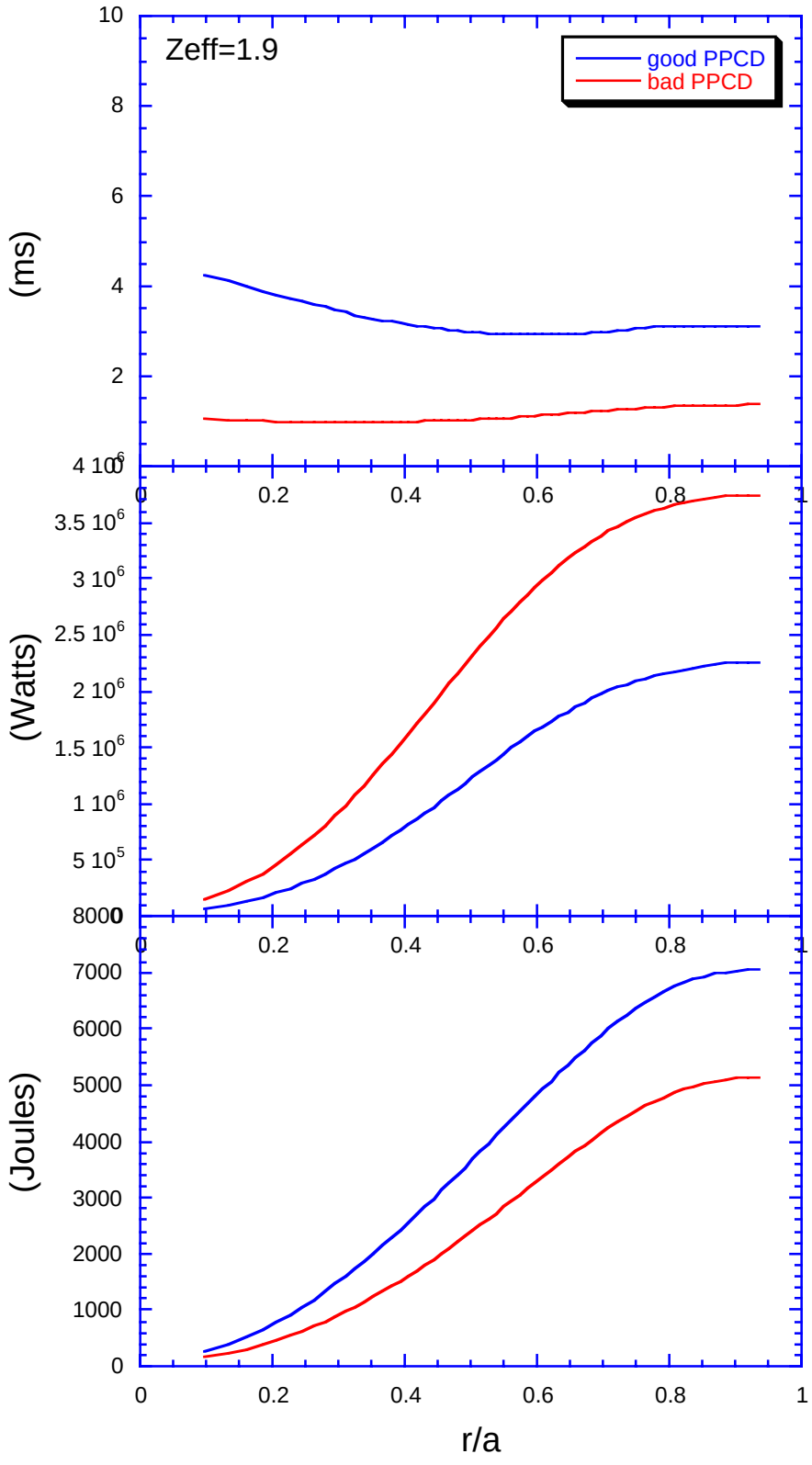

PPCD Leads to Lower Electron Thermal Conductivity

Ip~200 kA

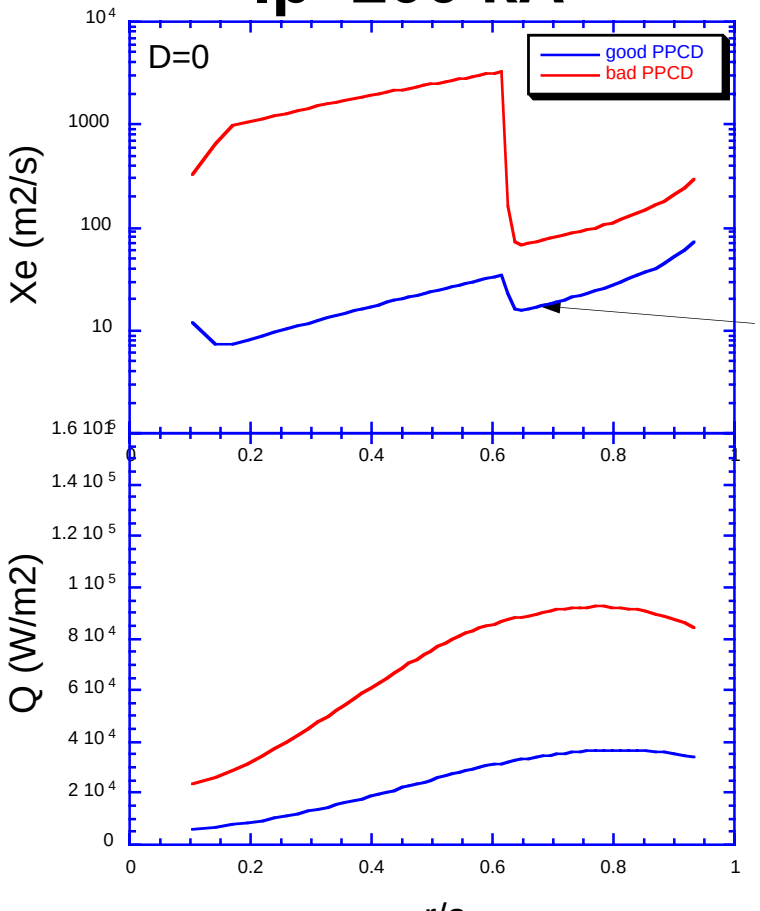

Xe is reduced by a factor of 100 in the core and by a factor of 5 at the edge.

Better Xe at the edge leads to an energy transport barrier for electrons.

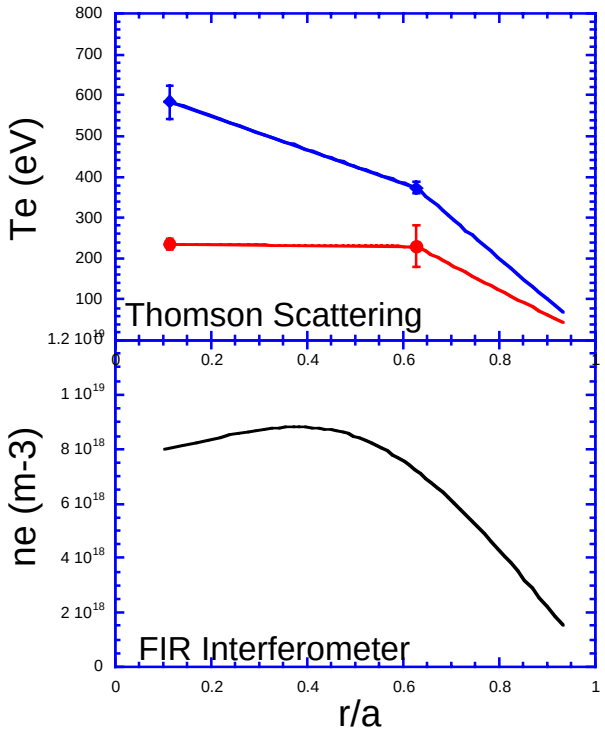

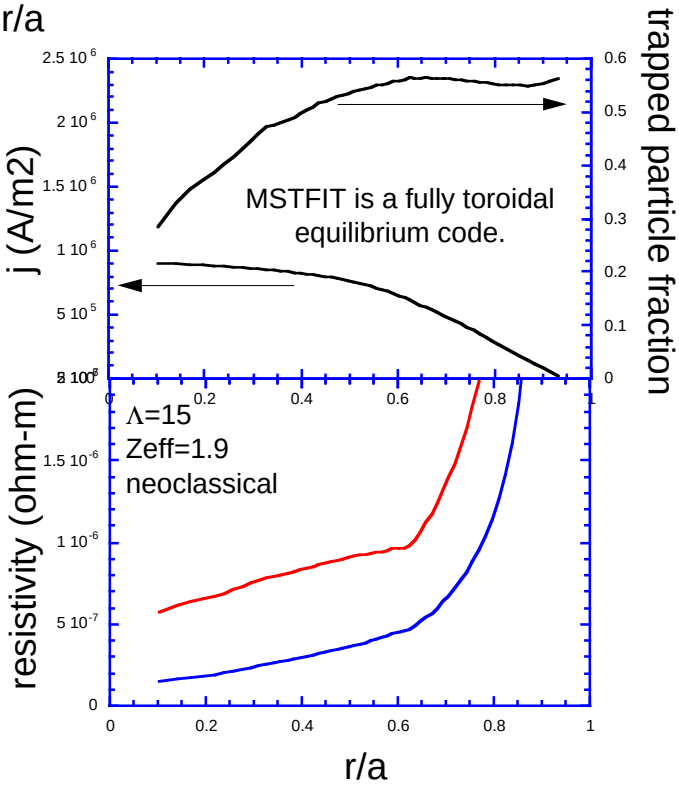

PPCD Increases Energy Confinement Time for Electrons to ~4 ms (w/est. ohmic power)

Ip~200 kA

Energy Confinement Time for electrons

$$\tau_{E,e} \approx \frac{\int \frac{3}{2} n_e T_e \frac{\partial V}{\partial r} dr}{\int \eta j^2 \frac{\partial V}{\partial r} dr}$$

Ohmic Input Power

$$\int \eta j^2 \frac{\partial V}{\partial r} dr$$

Stored Thermal Energy

$$\int \frac{3}{2} n_e T_e \frac{\partial V}{\partial r} dr$$

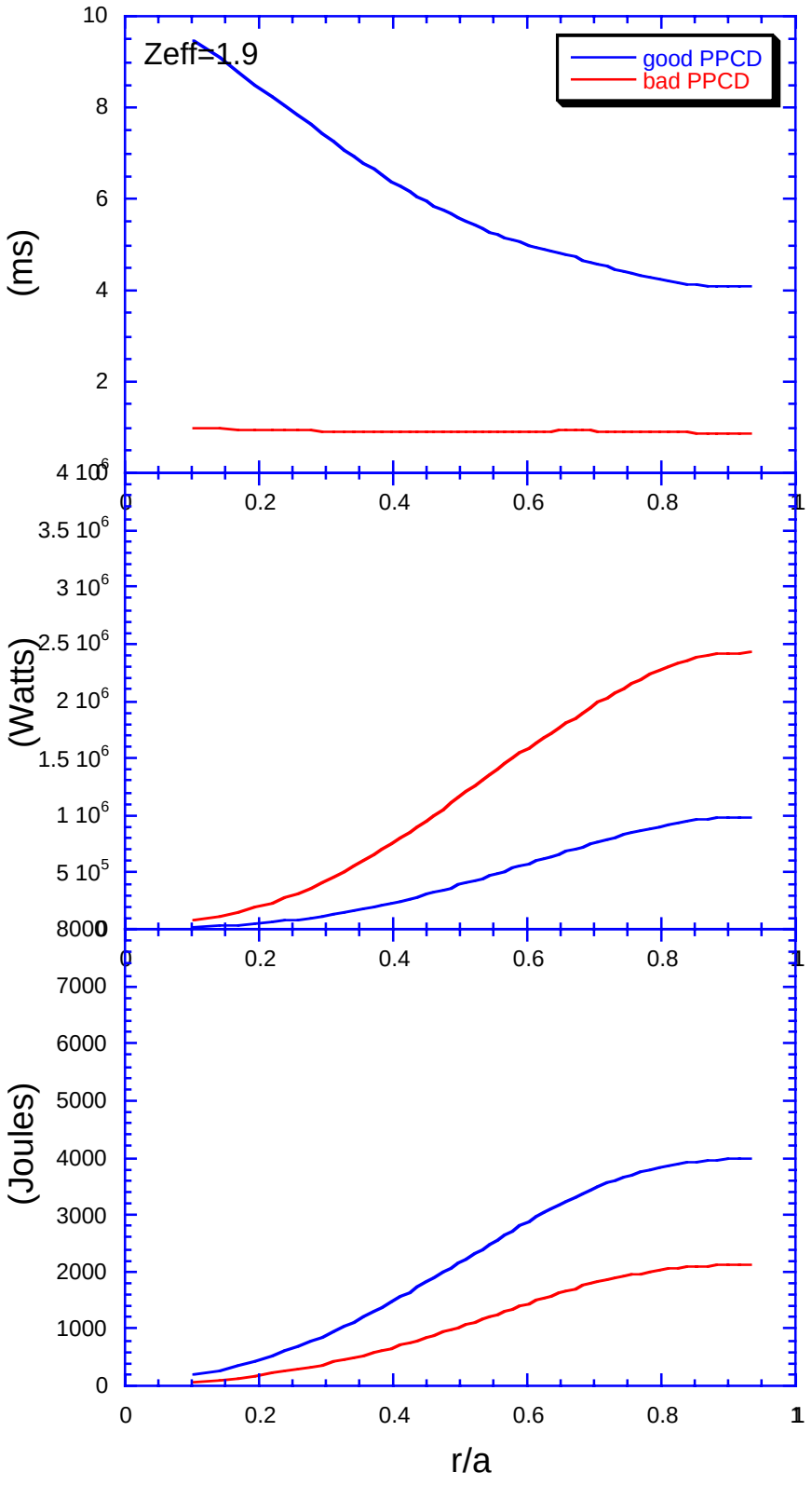

Local Power Balance Constrains D < ~10 m2/s for r/a > 0.8 (for a Zeff of 1.9)

Increasing the particle diffusion coefficient, D, results in unphysical Xe values.

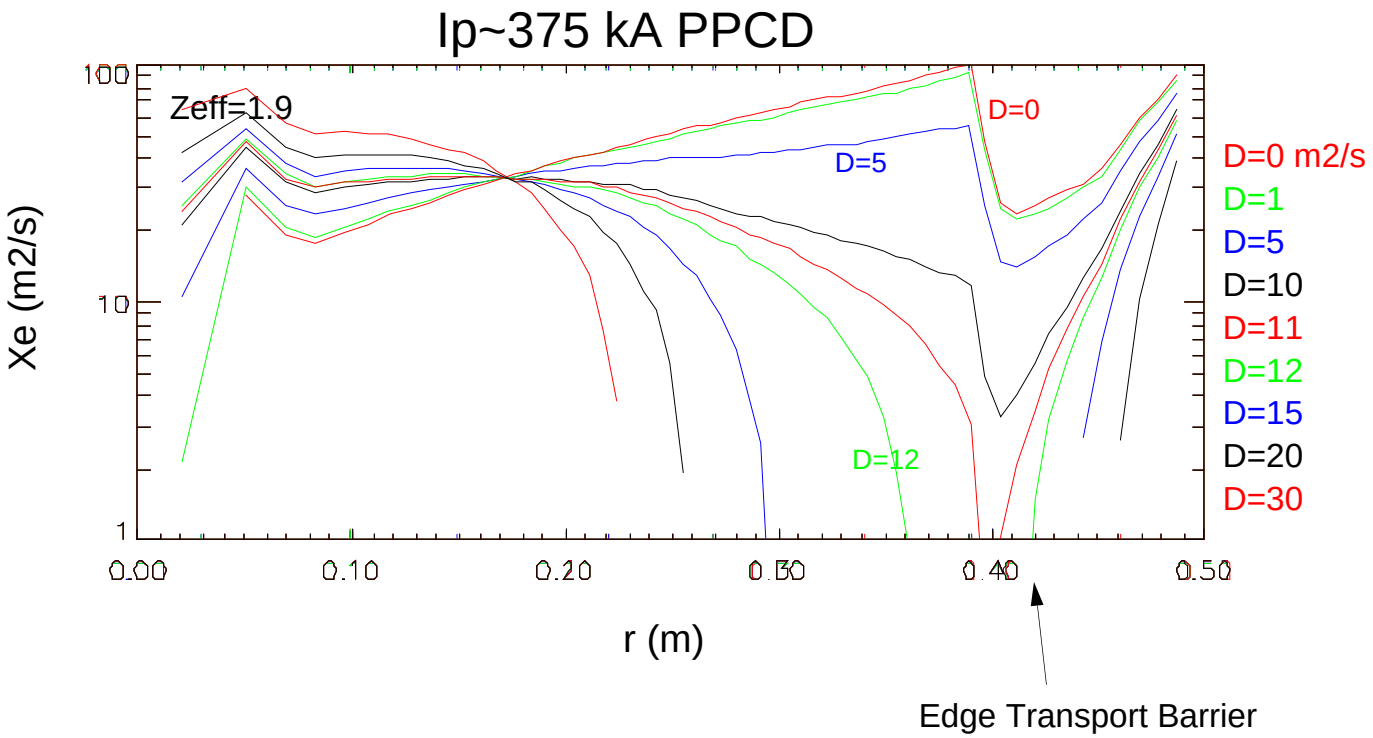

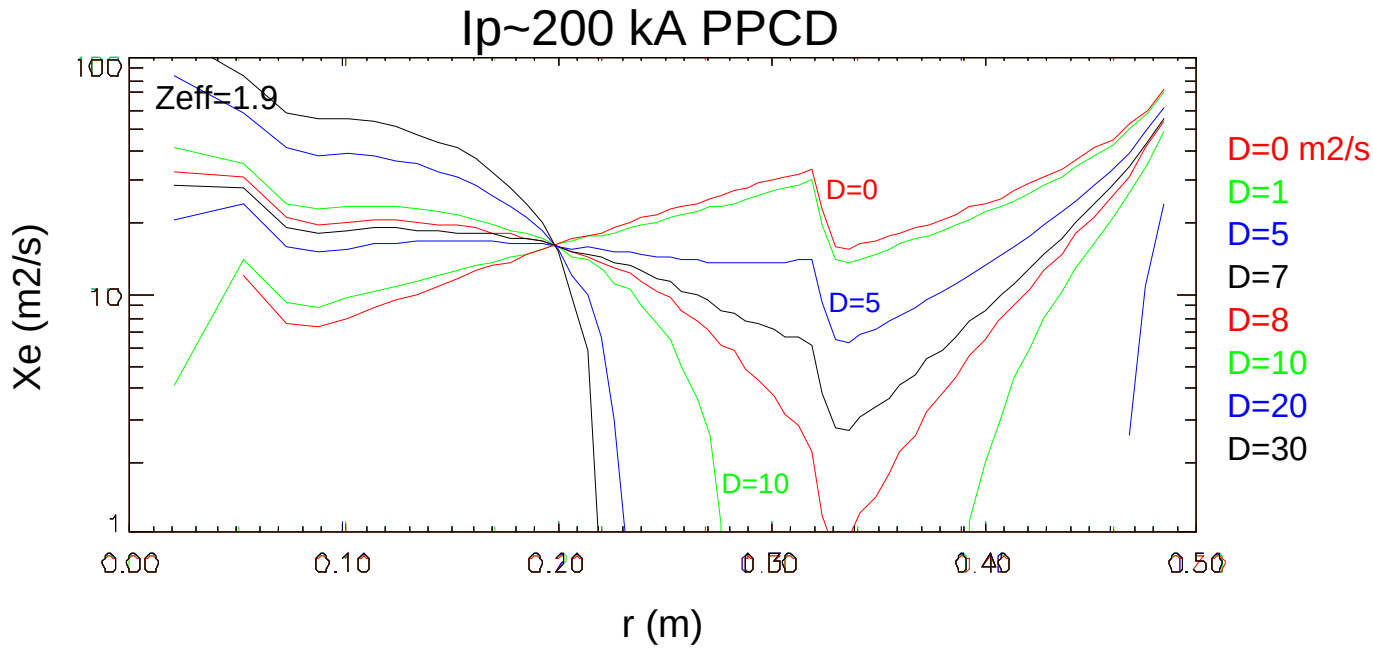

Increasing Zeff raises the Xe curves and allows a higher bound on D.

$\tau_{E,e}$ in the MST during PPCD probably reaches ~4 ms

Ip~375 kA

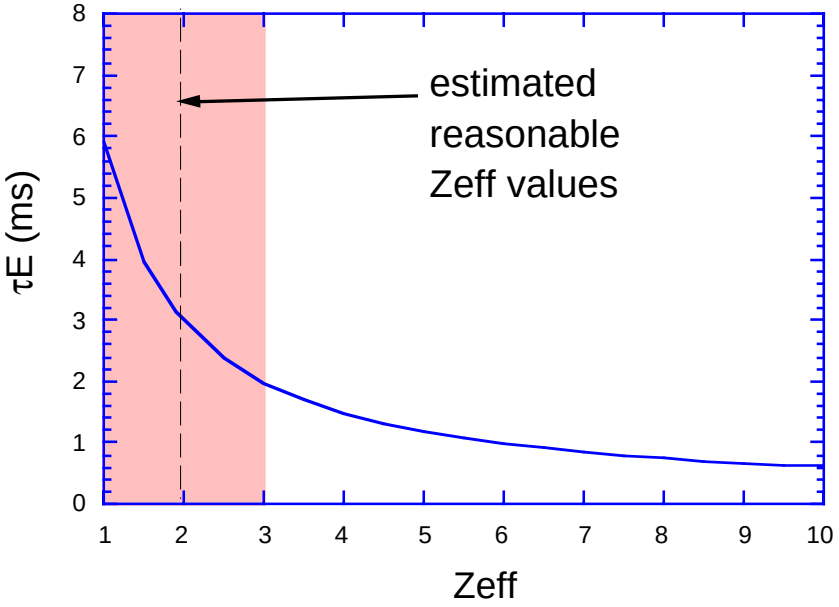

Ip~200 kA

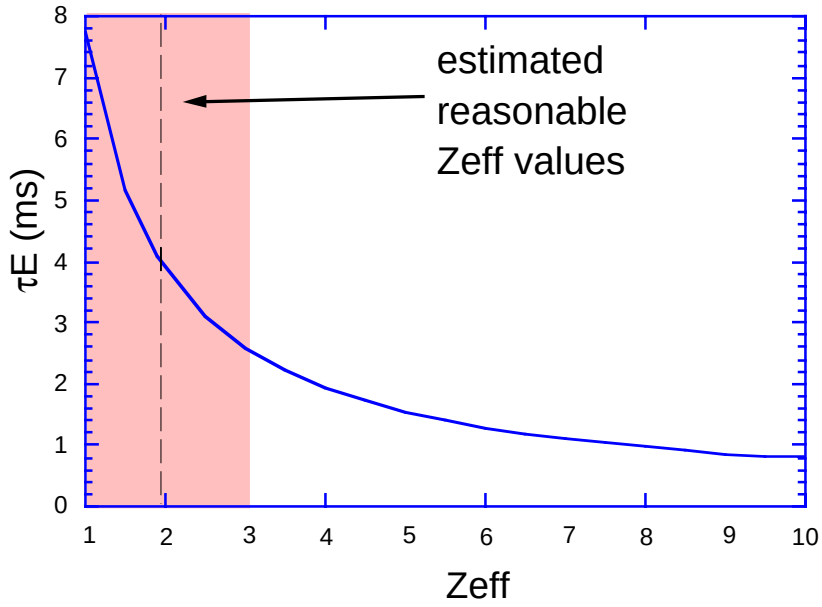

Tentatively,
For Zeff=1.9
τ_E=3.1 ms
and
$\beta_{p,e}$=6.7%

$$\beta_{p,e} = \frac{p_{plasma}}{p_{magnetic}} = \frac{\frac{1}{V}\int n_e T_e dV}{\frac{1}{2\mu_0} B_p^2}$$

Tentatively,
For Zeff=1.9
τ_E=4.1 ms
and
$\beta_{p,e}$=15%

These values represent a lower bound,including neoclassical trapped particle effects.

Energy Confinement Times in MST: a historical perspective

τ_E	conditions	Pohmic	$Z_{eff}^*=Z_{eff}/(1-f_t)$
~1 ms	MST "standard" 1996	measured $P_{ohmic}=P_{input}-P_{mag.}$	2.5
~5 ms	single pulse PPCD 1996	measured Pohmic=Pinput-Pmag.	1.7

Zeff was estimated by comparing α -model calculations of $\eta j2$ to measured P_{ohmic}. In this way Z* includes trapped particle corrections.

~4 ms	multi-pulse PPCD 1998	MSTFIT est.	1.9/(1-ft)

Pohmic could not be measured directly. Instead, Zeff was guessed to be1.9 based on NIRB measurements. MSTFIT modeling was used to calculate j and the trapped particle fraction (~0.55).

Energy confinement during PPCD in MST exceeds "Constant β" scaling at Ip = 200 kA.

- Electron poloidal beta $\beta_\theta \approx 15\%$ (electron total beta $\beta \approx 13\%$).
- Ohmic input power estimated from $\int \eta J^2 dV$ with measured electron temperature profile and toroidal equilibrium modeling (including ~2X trapped electron resistivity enhancement).

World RFP Confinement Database

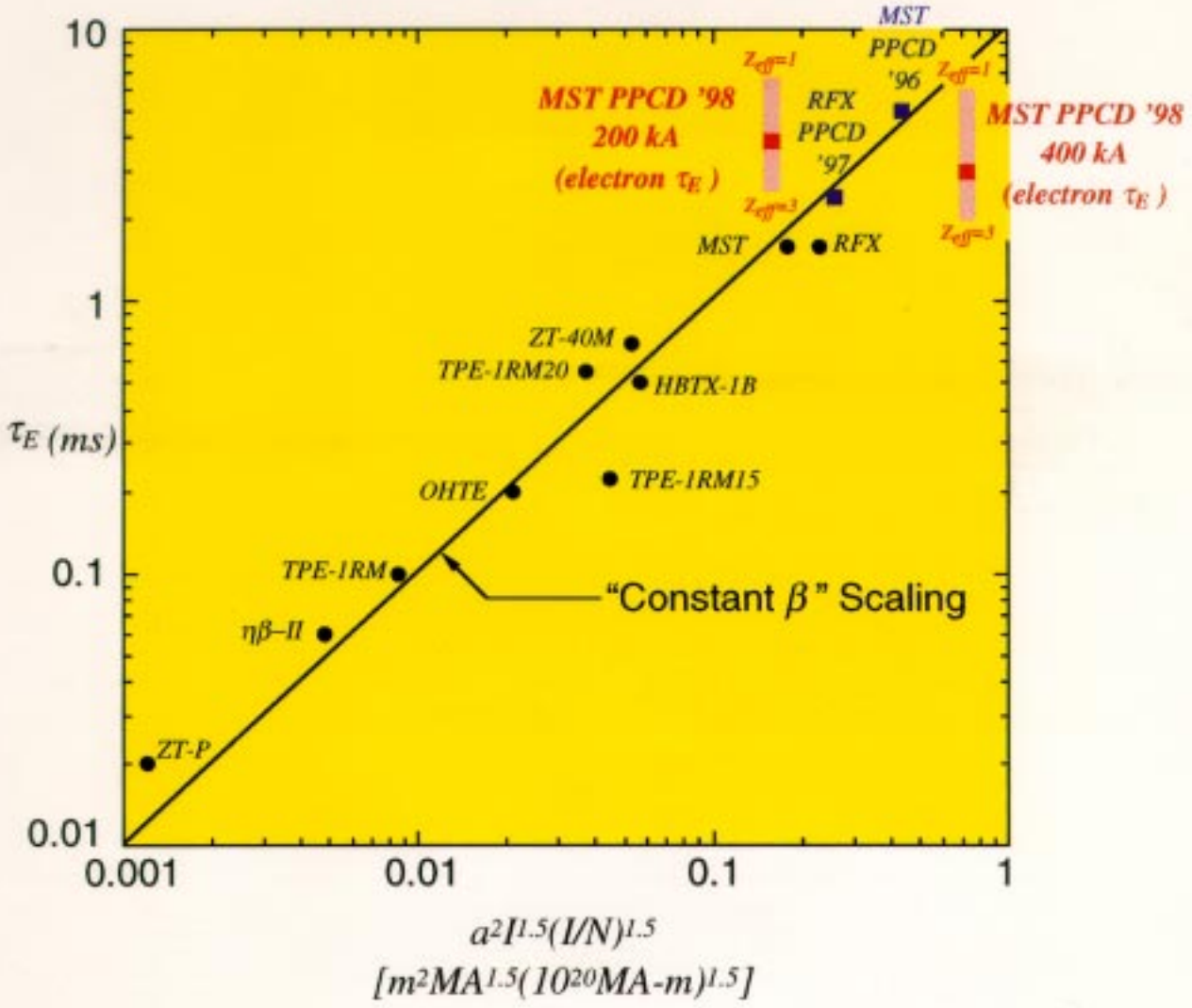

Conclusions

- For the first time, profiles of T_e have been measured during PPCD in the MST.

- **Local power balance constrains D < 10 m^2/s in the edge of MST during PPCD.** Energy transport can be fully accounted for in terms of conduction, rather than convection, based on the value of X_e.

- **X_e is lower in the edge than in the core, indicating an edge energy transport barrier**. PPCD lowers X_e in the core through a peaking of the T_e profile and consequently improves core confinement while edge confinement remains relatively unchanged.

- **The energy confinement time for electrons greatly improves during PPCD**, presumably due to the decrease in magnetic fluctuations.

  $\tau_{E,e}$**~4 ms** (if Z_{eff}~2) from 1 ms

- **$\beta_{p,e}$ reaches 15% during low current PPCD.**

Related Posters

Session F3P - Poster Session: RFPs and other Alternate Confinement Devices.

[F3P.05] The effects of small dynamo events and their suppression on enhanced confinement discharges in the MST RFP

B.E. Chapman, T.M. Biewer, C.-S. Chiang, D. Craig, P.W. Fontana, A.K. Hansen, D. Holly, N.E. Lanier, S.C. Prager, J.S. Sarff (University ofWisconsin-Madison)

[F3P.06] Electron Density Fluctuation Characteristics During Enhanced Confinement in MST

Y. Jiang, D.L. Brower (Electrical Engineering Department, University of California, Los Angeles), N.E. Lanier, A. Almagri, B.E. Chapman, C.-S. Chiang, D. Craig, G. Fiksel, S.C. Prager, J.S. Sarff (Department of Physics, University of Wisconsin, Madison)

[F3P.11] Interferometer and Polarimeter Measurements of Electron Particle and Current Transport in MST

N. E. Lanier, J. K. Anderson, C.B. Forest, D. J. Den Hartog, D. Holly, A. F. Knight, S. C. Prager (University of Wisconsin-Madison), D. L. Brower, Y. Jiang (University of California-Los Angeles)

[F3P.13] Evolution of Electron Density and Current Density Profiles During PPCD in MST

D.L. Brower, Y. Jiang (Electrical Engineering Department, University of California, Los Angeles), N.E. Lanier, D. Holly, J. Anderson, B.E. Chapman, C. Forest, S.C. Prager, J.S. Sarff (Department of Physics, University of Wisconsin, Madison)